

Extension of the selection of protein chromatography and the rate model to affinity chromatography[†]

G. Sandoval^a, C. Shene^b, B. A. Andrews^a and J. A. Asenjo^{a*}

The rational selection of optimal protein purification sequences, as well as mathematical models that simulate and allow optimization of chromatographic protein purification processes have been developed for purification procedures such as ion-exchange, hydrophobic interaction and gel filtration chromatography. This paper investigates the extension of such analysis to affinity chromatography both in the selection of chromatographic processes and in the use of the rate model for mathematical modelling and simulation. Two affinity systems were used: Blue Sepharose and Protein A. The extension of the theory developed previously for ion-exchange and HIC chromatography to affinity separations is analyzed in this paper. For the selection of operations two algorithms are used. In the first, the value of η , which corresponds to the efficiency (resolution) of the actual chromatography and, Σ , which determines the amount of a particular contaminant eliminated after each separation step, which determines the purity, have to be determined. It was found that the value of both these parameters is not generic for affinity separations but will depend on the type of affinity system used and will have to be determined on a case by case basis. With Blue Sepharose a salt gradient was used and with Protein A, a pH gradient. Parameters were determined with individual proteins and simulations of the protein mixtures were done. This approach allows investigation of chromatographic protein purification in a holistic manner that includes ion-exchange, HIC, gel filtration and affinity separations for the first time. Copyright © 2010 John Wiley & Sons, Ltd.

Keywords: rational selection; affinity chromatography; mathematical; modelling

INTRODUCTION

Over the past years, we have developed a computer based expert system based on proteomic data of proteins for the rational selection of optimal protein purification sequences (Asenjo and Andrews, 2004), as well as mathematical models that simulate and allow optimization of chromatographic protein purification processes (Shene *et al.*, 2006). So far these systems have mainly considered more generic purification procedures such as ion-exchange, hydrophobic interaction and gel filtration chromatography. This paper investigates the extension of such analysis to affinity chromatography both in the selection of chromatographic processes and in the mathematical modelling and simulation of chromatographic performance.

Expert system on proteomic data for the selection of protein purification

A clear rationale for the selection of high-resolution purification operations has been previously developed (Asenjo and Andrews, 2004). It characterizes the ability of the separation operation to separate one protein from another by using the theoretical concept of separation coefficients (SC) (Asenjo, 1990; Leser and Asenjo, 1992). It uses a relationship between the separation coefficient ($SC = DF \times \eta$) and the variables that determine the performance in a separation process: the deviation factor (DF) for differences among physicochemical properties and the efficiency (η) of the process. The DF was defined as the difference in a particular physico-chemical property (such as molecular weight, charge or hydrophobicity) between two proteins, which

correspond to the target protein and the particular contaminant protein being considered (Asenjo and Andrews, 2004). To include the rule-of-thumb that reflects the logic of first separating impurities present in higher concentrations, a relative contaminant protein concentration (θ), and the selection separation coefficient (SSC) is defined as the product of the SC and this relative concentration ($SSC = SC \times \theta = DF \times \eta \theta$). The relationship between the SC and resolution and efficiency has been described in detail previously (Asenjo and Andrews, 2004).

Two basic algorithms were developed in order to choose the optimal sequence of operations to use in a protein purification process. In the first algorithm the SSC between the target protein and each of the main contaminant proteins for each of the physico-chemical properties is calculated and the values of all the

* Correspondence to: J. A. Asenjo, Centre for Biochemical Engineering and Biotechnology, Institute for Cell Dynamics and Biotechnology: a Centre for Systems Biology, University of Chile, Beauchef 850, Santiago, Chile
E-mail: juasenjo@ing.uchile.cl

a G. Sandoval, B. A. Andrews, J. A. Asenjo
Centre for Biochemical Engineering and Biotechnology, Institute for Cell Dynamics and Biotechnology: a Centre for Systems Biology, University of Chile, Beauchef 850, Santiago, Chile

b C. Shene
Department of Chemical Engineering, University of La Frontera, Temuco, Chile

[†] This article is published in *Journal of Molecular Recognition* as a special issue on Affinity 2009, edited by Gideon Fleminger, Tel-Aviv University, Tel-Aviv, Israel and George Ehrlich, Hoffmann-La Roche, Nutley, NJ, USA.

SSCs is ordered in decreasing order. The operation and conditions that give the largest value of SSC is then chosen as the first separation (chromatography) to use.

A second algorithm was developed to modify the protein concentrations in the database of contaminants of those that have either been totally eliminated or diminished after the first separation process is performed. The amount of a protein contaminant eliminated after a chromatographic step was carried out by simplifying the shape of the chromatographic peaks to a narrow triangle (Asenjo and Andrews, 2004). A variable, Σ , corresponds to the peak width and has been experimentally determined (Lienqueo *et al.*, 1996) and it was found that under the conditions normally used for protein purification, the value of Σ is virtually independent of protein concentration.

Affinity chromatography was not considered in any rational manner as part of the heuristics of this process. It was assumed that if this technique is chosen by the user all contaminants will be reduced by a fixed percentage (e.g. 90%) in the affinity separation step (Leser, 1996). However, since affinity chromatography will have to be analyzed on a case by case basis, given the nature of the different ligands that can be used (e.g. metal ions in IMAC, dye or other) it was not included in the Expert System.

Mathematical modelling to simulate chromatography

Once the type of chromatography is chosen, optimization of the operating conditions is essential. In chromatography, protein adsorption depends on composition and concentration of the mixture and also on operational conditions such as flow rate, ionic strength gradient, sample load, physical properties of the adsorbent matrix and column dimensions. Mathematical models for describing a chromatographic separation have been discussed previously (Shene *et al.*, 2006; Orellana *et al.*, 2009). Two such models are the plate model and the more fundamentally based rate model.

The plate model is based on the plate theory. The model assumes that the chromatographic column is formed by a number of plates (N_p) each of them having the same ratio between the stationary phase volume and the volume of the mobile phase (H). For a defined column geometry and if the adsorption kinetics is known the problem is reduced to solve the system of N_p ordinary differential equations (ODE). In order to solve this ODE system the ionic strength at each plate ($i = 1 \dots N_p$) has to be computed as a function of time.

In the more fundamentally based rate model the dimensionless elution curves are obtained from the solution of a partial differential equation (PDE) subject to the initial and boundary conditions. In order to solve the PDE the dimensionless concentration profile for each component in the liquid phase contained inside the particles, c_p , has to be computed. These concentration profiles are obtained from the solution of another PDE also subject to initial and boundary conditions.

Since all mass transfer phenomena are taken into account in the PDEs, rate models can be used for testing different chromatographic conditions (Gu, 1995; Lazo, 1999).

The rate model has recently been applied to very high protein concentrations (up to *ca.* 40 g/L) such as those found in many practical and large-scale industrial applications. (Orellana *et al.*, 2009). With pure proteins at high concentrations the model could simulate changes in flow rate, ionic strength, salt gradient and separation time. When protein mixtures at high concentrations

were simulated some of the kinetic parameters of the individual proteins had to be modified to take into account protein–protein interactions, competition and displacement. In this way the model allowed prediction of the behaviour of the elution curves as a function of flow rate, ionic strength and salt gradient with a relative error below 5%. Li *et al.* (2004), developed a similar model for dye–ligand affinity chromatography using a binary adsorption isotherm.

A mathematical function was built that included parameters to optimize protein production as well as the effects of chromatography performance such as yield, purity, concentration and the time needed to accomplish the separation (Shene *et al.*, 2006; Orellana *et al.*, 2009). Operational conditions in the chromatography such as flow rate, ionic strength gradient and the operational time can be selected using the model to optimize the protein production process depending on the characteristics of the final product such as purity and yield. This mathematical function was successfully used for the selection of the operational conditions as well as the fraction of the product to be collected (peak cutting) in a chromatographic operation.

The aim of this paper is to investigate the extension of such successful analyses to affinity chromatography both in the selection of chromatographic processes and in the mathematical modelling and simulation of chromatographic performance.

MATERIALS AND METHODS

The high-performance liquid chromatography system employed consisted of a fast protein liquid chromatography (FPLC) System (GE Healthcare, Uppsala, Sweden) equipped with a 100 and 500 μ L injection loop. The chromatographic columns were a Blue Sepharose CL-6B matrix (Sigma R9903) packed into a 5/5 column HR (5 cm length, 0.5 cm diameter, Pharmacia Biotech) and a HiTrap rProtein A FF (1 mL, GE Healthcare 17-5079-02). The experiments were performed at room temperature, using flow-rates equal to 0.1 mL/min for the dye–ligand experiments and 1 and 3 mL/min for the Protein A affinity experiments.

For the dye–ligand affinity chromatography two proteins were used: haemoglobin (Hb) from rabbit (Sigma H7255) and albumin from bovine serum albumin (BSA, Sigma A7030) in a buffer 10 mM Tris–HCl containing 0.05 M NaCl (pH 7.5). To elute components retained in the column, a linear gradient of salt concentration was created using a buffer 10 mM Tris–HCl containing 1 M NaCl at pH 7.5. The gradient molarity was estimated from the conductivity of the solution. The elution curve of Hb as a function of time was directly obtained from the measurements of absorbance at 405 nm of the outlet flow, while the elution curve of BSA was obtained from the measurements of absorbance at 280 nm by subtracting the contribution of Hb at that wavelength.

For the Protein A affinity chromatography three proteins, with different affinity for the Protein A were used: Mouse IgG1 (Sigma M5284), Mouse IgG2a (Sigma M5409) and Mouse IgG2b (Sigma M5534) in a buffer 20 mM sodium phosphate at pH 7.0. A pH linear gradient was created for the elution of the retained components using a buffer 0.1 M sodium citrate at pH 3.0. The pH gradient was directly measured with a pH electrode and the elution curves were obtained from the measurements of the absorbance at 280 nm of the outlet flow as a function of time.

In order to adjust the adsorption kinetic parameters and to transform the absorbance measurements into concentration

Table 1. Operating conditions for pure proteins used in the experimental runs

	Dye-ligand	Protein A
Flow (mL/min)	0.1	1
Injection volume (μL)	500	100
Protein Concentration (mg/mL)	1	0.15
Length of the linear gradient (CV)	5.5	10

values, experiments for pure proteins were carried out for both chromatographic systems using the conditions shown in Table 1.

MATHEMATICAL MODEL FOR AFFINITY

The general rate model is based on mass balances and mass transfer phenomena that take place in affinity chromatography. This was formulated with the same assumptions made in the ion-exchange chromatography, IEC, model (Shene *et al.*, 2006; Orellana *et al.*, 2009), i.e. $t=0$ corresponds to the moment at which the sample is pumped to the column, radial dispersion effects for components in the mobile phase are null, and adsorbent particles (particles from now on) are assumed spheres of uniform radii (R_p). In the present model it was assumed that properties of the stagnant phase (ionic strength and pH) inside the adsorbent particles are those of the mobile phase that surround them (no gradients).

In the column, protein in the mobile phase moves due to dispersion and convective flow; it is also transported inside the particles. Because at different axial positions protein concentration at the surface of particles is different, solution of the mass balance equation for the protein in the mobile phase must be coupled to the solution of mass balance applied to the particles. These two mass balances are given by PDEs because of the position and time dependent nature of the chromatographic process. Rate models for IEC, hydrophobic interaction chromatography and gel permeation chromatography are given by the same equations. For the first two processes differences are found in the adsorption kinetics or the relationship between adsorption rate constants and properties of the mobile phase.

Proteins are adsorbed onto the attached ligand according to a reversible reaction with rate constants for the adsorption and desorption kinetics equal to k_{ai} and k_{di} respectively:



Adsorption rate depends on the concentration of available sites for adsorption (L_a); this concentration is given by the difference between adsorption capacity (C^∞) and the sites occupied by adsorbed proteins ($\sum_{i=1}^N C_i^*$). Accordingly, changes in concentration of adsorbed proteins (C_i^*) are given by,

$$\frac{\partial C_i^*}{\partial t} = k_{ai} C_i \left(C_i^\infty - \sum_{i=1}^N C_i^* \right) - k_{di} C_i^* \quad (2)$$

At steady state, the relationship in (2) reduces to the Langmuir isotherm for multicomponents. Our model assumes that properties of the mobile phase (C_{N+1}) affect the desorption rate

constant and its contribution is to model this effect through simple relationships (Eqs. 3a and b):

$$\text{For pH gradient : } k_{di} = \alpha'_i e^{\beta'_i (C_0/C_{N+1, \max} - C_{N+1}/C_{N+1, \max})} \quad (3a)$$

$$\text{For ionic strength gradient :} \quad (3b)$$

$$k_{di} = \alpha'_i e^{\beta'_i (C_{N+1}/C_{N+1, \max} - C_0/C_{N+1, \max})}$$

Parameters α'_i and β'_i for each protein depend on the protein-adsorbent affinity and the conditions used for the elution (pH or ionic strength). C_0 is the initial ionic strength or pH of the mobile phase. The relationships proposed for the desorption rate constant permit an important increase once the ionic strength or pH in the mobile phase reaches the value at which protein affinity to the adsorbent is reduced.

The following equations in the model (4–7) are the same as those found in the IEC rate model (Shene *et al.*, 2006; Orellana *et al.*, 2009). The PDE for each protein ($i=1 \dots N$) in the mobile phase corresponds to:

$$-D_{bi} \frac{\partial^2 C_{bi}}{\partial Z^2} + v \frac{\partial C_{bi}}{\partial Z} + \frac{\partial C_{bi}}{\partial t} + \frac{3k_i(1-\varepsilon_b)}{\varepsilon_b R_p} (C_{bi} - C_{pi, R=R_p}) = 0 \quad (4)$$

In this PDE, the first and second terms represent transport of protein i by axial dispersion and convective flow, respectively, where D_{bi} is the dispersive coefficient and v velocity of the mobile phase through the bed. The fourth term in the PDE in relationship (4) is the mass transfer flux from the mobile phase to the particle surface, in which k_i is the mass transfer coefficient, and ε_b the bed porosity. For ionic strength and pH ($i=N+1$) the fourth term in this PDE was not considered due to the assumption of no gradient inside the particle for these components. At the column inlet ($Z=0$), protein dispersion flux equals the input mass flux, thus:

$$D_{bi} \frac{\partial C_{bi}(t, 0)}{\partial Z} = v [C_{bi}(t, 0) - C_{Fi}(t)] \quad (5)$$

At the column outlet ($Z=L$), protein dispersion flux is null ($D_{bi}(\partial C_{bi}/\partial Z) = 0$).

The following PDE represents the mass balance for a protein in the stagnant phase inside a particle:

$$\frac{\partial C_i^*}{\partial t} + \varepsilon_p \frac{\partial C_{pi}}{\partial t} - \varepsilon_p D_{pi} \left[\frac{1}{R^2} \frac{\partial}{\partial R} \left(R^2 \frac{\partial C_{pi}}{\partial R} \right) \right] = 0 \quad (6)$$

The third term represents protein diffusion through the stagnant fluid phase that could become adsorbed onto the particle surface or desorbed from it depending on the properties of the fluid phase (first term). At the centre of the particle ($R=0$) symmetry conditions hold ($(\partial C_{pi}/\partial R) = 0$). The changes in the mobile phase and those taking place inside the particles are related because the diffusional flux to the particle and the mass transfer flux from the mobile phase must be equal, thus,

$$\varepsilon_p D_{pi} \frac{\partial C_{pi}(t, R_p, Z)}{\partial R} = k_i [C_{bi}(t, Z) - C_{pi}(t, R_p, Z)] \quad (7)$$

In solving PDEs the computations can almost always be simplified by the use of dimensionless variables. By using the dimensionless variables $c_{bi} = C_{bi}/C_{oi}$, $c_i^* = C_i^*/C_{oi}$, $\tau = tv/L$, $r = R/R_p$, $z = Z/L$, coefficients in the PDEs in (4) and (6) are given in terms of the following dimensionless numbers, Peclet number ($Pe_i = vL/D_{bi}$), Biot number ($Bi_i = K_i R_p / [\varepsilon_p D_{pi}]$), $\pi \varepsilon_p D_{pi} L / (R_p^2 v)$, $\xi_i = 3Bi_i \pi (1-\varepsilon_b) / \varepsilon_b$, and Damköhler numbers for adsorption $Da_i^a = L \times k_{ai} C_{oi} / v$ and, desorption $Da_i^d = L \times k_{di} / v$.

Dimensionless model equation for the components of the mobile phase are,

$$\text{Proteins : } -\frac{1}{\text{Pe}_L} \frac{\partial^2 c_{bi}}{\partial z^2} + \frac{\partial c_{bi}}{\partial z} + \frac{\partial c_{bi}}{\partial \tau} + \xi_i (c_{bi} - c_{pi,r=1}) = 0 \quad (8a)$$

$$\text{Ionic strength or pH : } -\frac{1}{\text{Pe}_L} \frac{\partial^2 c_{bN+1}}{\partial z^2} + \frac{\partial c_{bN+1}}{\partial z} + \frac{\partial c_{bN+1}}{\partial \tau} = 0 \quad (8b)$$

For the proteins in the particles,

$$(1 - \varepsilon_p) \frac{\partial c_i^*}{\partial \tau} + \varepsilon_p \frac{\partial c_{pi}}{\partial \tau} - \pi \left[\frac{1}{r^2} \frac{\partial}{\partial r} \left(r^2 \frac{\partial c_{pi}}{\partial r} \right) \right] = 0 \quad (9)$$

For the adsorption kinetics

$$\frac{\partial c_i^*}{\partial \tau} = \text{Da}_i^a c_{pi} (c_i^\infty - c_i^*) - \text{Da}_i^d c_i^* \quad (10)$$

with, $\text{Da}^d = \alpha_i e^{\beta_i(c_{0,N+1} c_{N+1})}$ and $\text{Da}^a = \alpha_i e^{\beta_i(c_{N+1} - c_{0,N+1})}$ when a pH gradient or ionic strength gradient is used for protein elution, respectively. The dimensionless boundary conditions in (5) and (7) are given by:

$$\begin{aligned} \frac{\partial c_{bi}(\tau, 0)}{\partial z} &= \text{Pe}_L \left[c_{bi}(\tau, 0) - \frac{C_{Fi}(\tau)}{C_{0i}} \right] \\ \frac{\partial c_{pi}(\tau, 1, z)}{\partial r} &= \text{Bi}_i [c_{bi}(\tau, z) - c_{pi}(\tau, z, 1)] \end{aligned} \quad (11)$$

Protein concentration in the mobile phase that enters the column (C_F) is given by:

$$\frac{C_{F,i}(\tau)}{C_{0i}} = \begin{cases} 1 & 0 \leq \tau \leq \tau_1 \\ 0 & \tau > \tau_1 \end{cases} \quad i = 1 \dots N_p \quad (12)$$

where τ_1 is the dimensionless time it takes to pump the sample. Changes in pH or ionic strength of the mobile phase are given by:

$$\frac{C_{F,N+1}(\tau)}{C_{0,N+1}} = \begin{cases} 0 & 0 \leq \tau \leq \tau_{\text{wash}} \\ a + b(\tau - \tau_{\text{wash}}) & \tau_{\text{wash}} < \tau \leq \tau_{\text{elution}} \\ c\tau & \tau > \tau_{\text{elution}} \end{cases} \quad (13)$$

During the interval $[\tau_1, \tau_{\text{wash}}]$ the nonadsorbed components retained inside the adsorbent particles, are eluted; after this and during $[\tau_{\text{wash}}, \tau_{\text{elution}}]$ elution pH or ionic strength change according to the gradient steepness b .

The model was solved numerically using Matlab. The finite element (with quadratic elements) and the orthogonal collocation methods were used to discretize the partial bulk-phase and particle-phase differential equations, respectively. The resulting ODE system was solved using ode15s routine in Matlab. Simulations were carried out on a personal computer with Windows 2000 operating system. Ten quadratic elements were used for discretizing the axial dimension and two for the radial dimension. Three parameters in the model equations for proteins (Pe , Bi , π) were calculated and three (Da^a , α and β) were estimated from experimental elution curves; Pe number for the ionic strength and pH were estimated separately from experimental curves. A genetic algorithm code (Carroll, 2009) was implemented in Matlab and was used to fit parameters in order to minimize the sum of squared differences between experimental and computed values of protein concentrations and pH or ionic strength. Estimated parameters for single protein were used to simulate elution curves of single proteins at conditions different from those used for parameter estimation and also to simulate the elution curve of protein mixtures.

RESULTS AND DISCUSSION

Selection of operation

The rationale for selection of high-resolution purification is based both on the differences in the physico-chemical property of the proteins (product and contaminant) being exploited in that particular chromatography (DF) and on the efficiency of the actual chromatography (η). In order to include affinity to a particular ligand in the already well-developed database of molecular weight, charge at different values of the pH and hydrophobicity we have tested two relatively standard affinity ligands which are Blue Sepharose and Protein A. In the same way the efficiency η , was characterized previously for ion-exchange, gel filtration and HIC (Asenjo and Andrews, 2004) this was done for these two ligands. Typical chromatograms are shown in Figure 1 for Blue Sepharose and in Figure 2 for Protein A. The values of the efficiency obtained are shown in Table 2 together with those previously obtained for ion-exchange, HIC and Gel Filtration. This parameter is essential for the application of the first algorithm of the methodology as has been explained in the introduction. In the affinity chromatography carried out with Blue Sepharose values close to 0.7 were found for the value of the efficiency whereas for Protein A, values in the range 0.9–1.0 were found. Hence the values obtained depend on the type of affinity system used and cannot really be considered as more 'generic' as

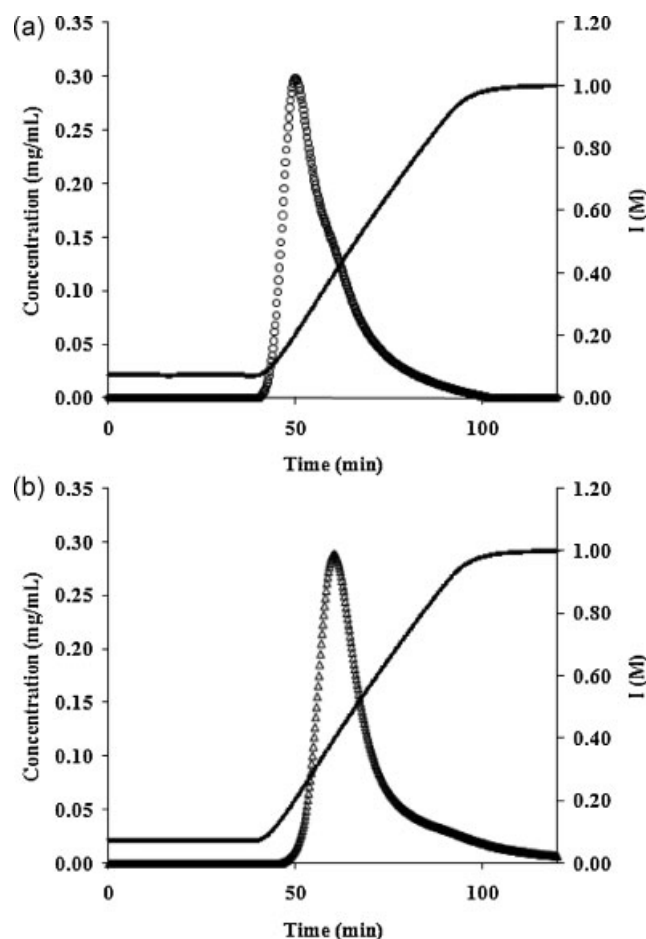


Figure 1. Typical chromatograms with Blue Sepharose with linear gradient of salt. (a) Hb and (b) BSA.

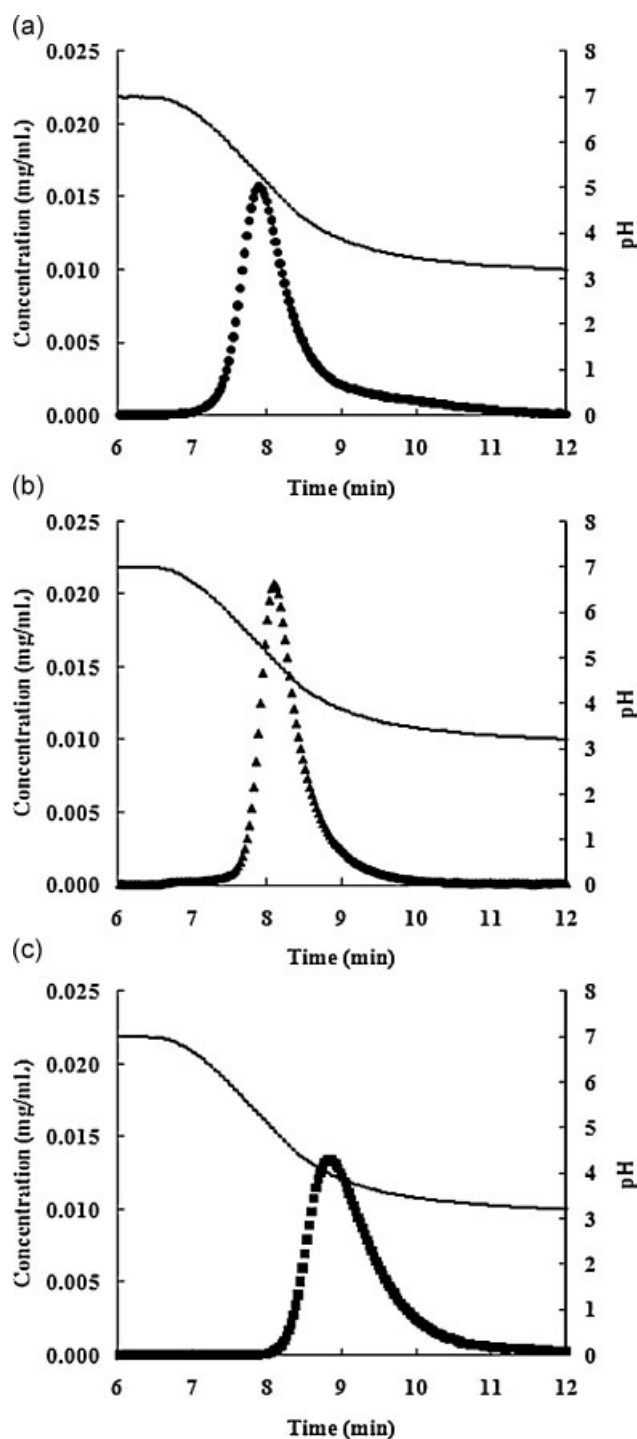


Figure 2. Typical chromatograms of IgG's with Protein A as ligand and a linear pH gradient. (a) IgG1, (b) IgG2a and (c) IgG2b.

was the case for ion exchange, HIC and gel filtration. For Protein A, even though the pH gradient cannot be as closely controlled to the desired linear behaviour as the salt gradient as can be clearly observed in Figures 1 and 2, the resolution obtained (η) is higher (0.9–1.0) than for Blue Sepharose (0.7). Hence, contrary to common belief, the high affinity Protein A matrix gave resolutions close to ion-exchange chromatography but not higher, and Blue Sepharose gave resolutions clearly lower than ion-exchange and even somewhat lower than HIC.

Table 2. Efficiency (η) obtained in this work for affinity chromatography compared with previous work

Chromatography	Efficiency (η)
Ion-exchange	1.00
Affinity: Blue Sepharose and Protein A	0.70–1.00
Hydrophobic interaction	0.86
Gel filtration	0.66

The second algorithm calculates and modifies how much of each of the protein contaminants is eliminated in each separation step. This is done by approximating the peaks to narrow triangles and the parameter Σ has to be found which corresponds to the width of the triangle at the base (Asenjo and Andrews, 2004).

This was done for both affinity ligands and the values of Σ obtained are shown in Table 3. Similarly to the determination of η , the value obtained for Σ depends on the type of affinity system used and would therefore have to be determined on a case by case basis for the specific type of affinity system used. Similarly to the calculation of the efficiency (η), the value obtained for the peak width (Σ) is much narrower for Protein A (0.22) than for Blue Sepharose (0.31) giving a higher resolution for Protein A. In this case the value of Σ for Protein A was not as narrow as for ion-exchange (Table 3) but similar to HIC, whereas the value for Blue Sepharose (dye–ligand) was between that obtained previously for HIC and gel filtration.

Modelling and simulating affinity

As described in the Materials and Methods Section and in the Mathematical Modelling Section, the two standard affinity ligands, Blue Sepharose and Protein A were investigated in order to assess the fitting and simulation of the mathematical model to the behaviour of specific proteins in these two materials, particularly since the elution strategy of the first one uses a salt gradient and the elution strategy of the second one uses a pH gradient or a pH step.

Blue Sepharose and salt gradient

Elution curves of BSA and Hb which have different affinities to Blue Sepharose are shown in Figure 1. These experimental curves were used for parameter estimation and the results are presented

Table 3. Values of dimensionless peak width (Σ) obtained in this work for affinity chromatography compared with previous work

Chromatography		Dimensionless peak width (Σ)
Affinity (this paper)	Dye-ligand (blue Seph.)	0.31
	Protein A	0.22
Ion-exchange		0.15
Hydrophobic Interaction		0.22
Gel filtration		0.46

Table 4. Parameters in the rate model used for simulating elution curves by salt gradient using Blue Sepharose

Component	F (mL/min)	C_0 (mg/mL)	V_m (mL)	Grad (CV)	D_a	β	α	Pe	Bi	π
BSA	0.1	1	0.5	5.5	25.02	1.7609	104.11	395.26	39.45	0.1068
Hb	0.1	1	0.5	5.5	66.72	1.2810	147.51	395.26	37.15	0.2555
Salt		0.05						395.26	10.45	23.743

in Table 4. Simulated curves are also shown in Figure 3. The Pe, Bi and π were parameters calculated and α , β and D_a were fitted for each protein as shown in Figure 3. The values estimated for the parameters were used for simulating the elution curve of the

two protein mixture as shown in Figure 4a. Figure 4b shows a simulation and experimental results using a different salt gradient. The Hb peak in the model shows virtually no displacement in the elution time whereas the BSA peak shows

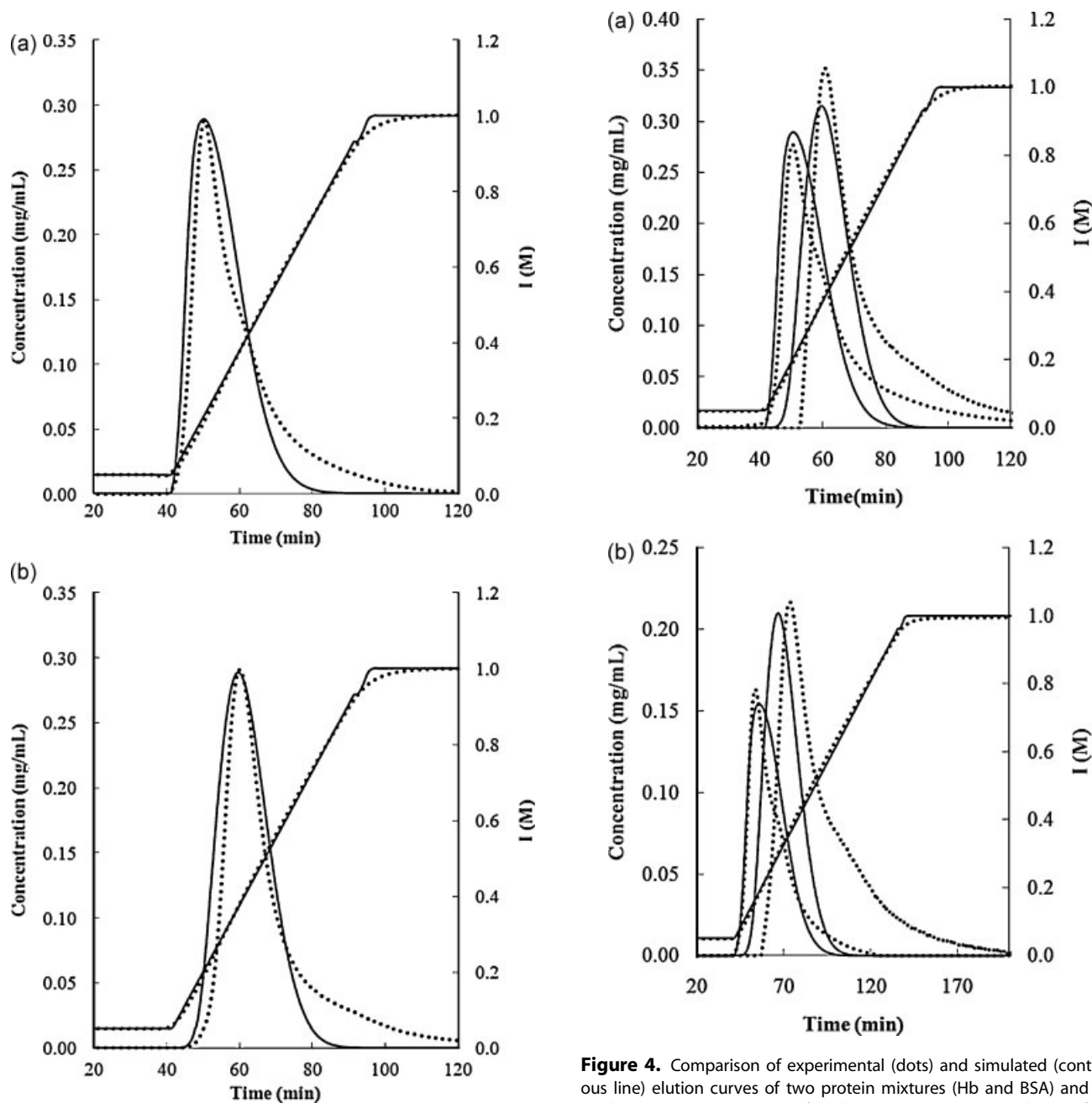


Figure 4. Comparison of experimental (dots) and simulated (continuous line) elution curves of two protein mixtures (Hb and BSA) and salt gradient, (a) concentration of both proteins 1 mg/mL, volume of the injection sample 500 μ L, flow rate 0.1 mL/min and gradient length 5.5 CV, (b) concentration of each protein 1 mg/mL, volume of the injection sample 500 μ L, flow rate 0.1 mL/min and gradient length 10 CV.

Figure 3. Comparison of experimental (dots) and simulated (continuous line) elution curves of (a) Hb and (b) BSA and salt gradient. Experimental data used for parameter estimation.

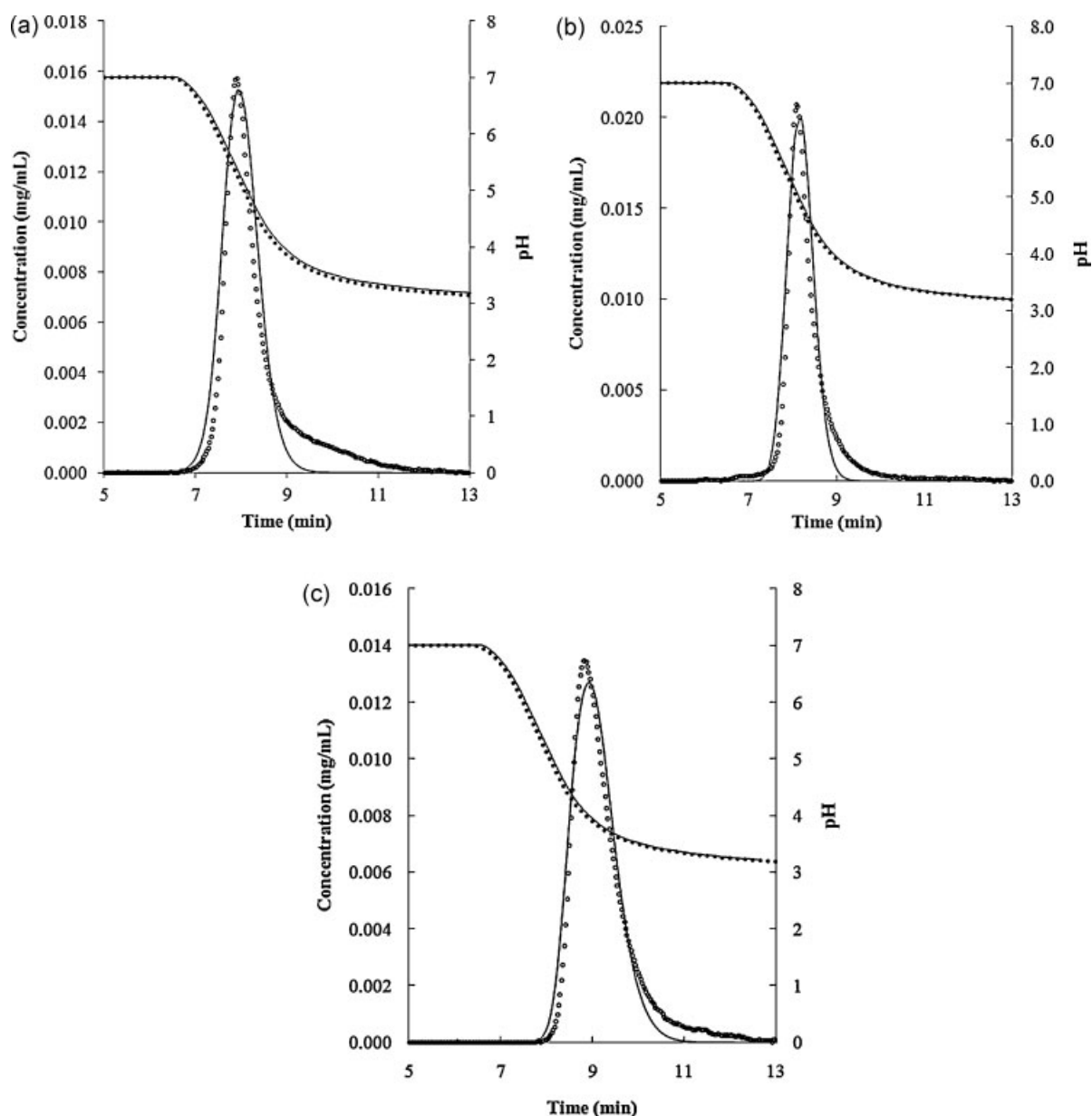


Figure 5. Comparison of experimental (dots) and simulated (continuous line) elution curves of (a) IgG1, (b) IgG2a, (c) IgG2b and pH gradient. Experimental data were used for parameter estimation.

an 8% displacement in Figure 4b. A similar small displacement for BSA was observed in the simulations of the model previously developed by Li *et al.* (2004). When comparing the experimental results and the model simulations for both Hb and BSA, a 'tail' can be observed in figures. Fig. 3a and b where the model does not follow the experimental results closely. Two explanations for this

behaviour could be that the experimental salt gradient does not follow the strictly linear gradient towards the end of the run and that the protein may not be totally homogeneous and that some glycosylation heterogeneity may be present in the sample used. This phenomena is also observed for the mixture of both proteins as can be seen in Figure 4a and b.

Table 5. Parameters in the rate model used for simulating elution curves by pH gradient using Protein A

Protein	F (mL/min)	C_0 (mg/mL)	V_m (mL)	Grad (CV)	Da	β	α	Pe	Bi	π
IgG1	1	0.149	0.1	10	0.1152	6.7116	5.8261	212.39	91.83	0.1691
IgG2a	1	0.149	0.1	10	0.2201	5.9780	9.5755	212.39	91.83	0.3711
IgG2b	1	0.149	0.1	10	1.5610	7.7755	7.3049	212.39	91.83	0.2426

Table 6. Operation conditions used for simulating elution curves of mixtures by pH gradient using Protein A shown in Figure 6

Mixture	Protein	Co (mg/mL)	F (mL/min)	V _m (mL)	Grad (CV)
a	IgG1	0.084	1	0.1	20
	IgG2b	0.095			
b	IgG1	0.016	1	0.25	20
	IgG2a	0.016			
c	IgG2a	0.038	1	0.1	20
	IgG2b	0.038			

Protein A and pH gradient

Elution curves of three IgGs (IgG1, IgG2a and IgG2b) with different affinities to Protein A are shown in Figure 5. These three experimental curves were used for parameter estimation; the results are presented in Table 5. The P_e , B_i and π were calculated

whereas α , β and D_a were fitted for each protein as shown in Figure 5. Simulated curves are also shown in the figures. Similarly to the behaviour shown for Blue Sepharose, the simulation results show a small difference with the experimental results for IgG1 and IgG2a in the tail of the peak (Figure 5a and b). This peak

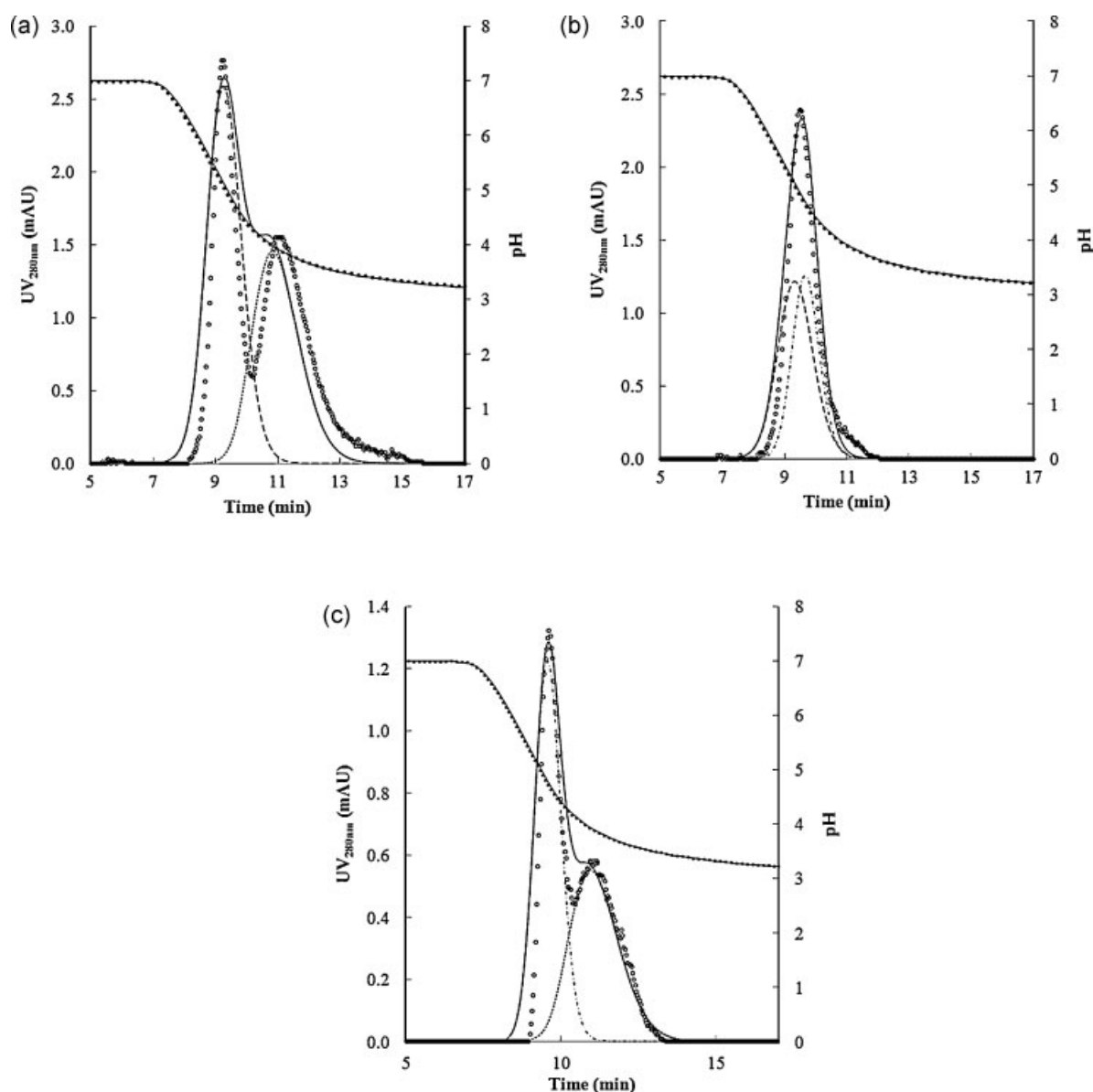
**Figure 6.** Comparison of experimental (dots) and simulated (continuous and semicontinuous lines) elution curves of various two protein mixtures (a) IgG1 and IgG2b, (b) IgG1 and IgG2a, (c) IgG2a and IgG2b and pH gradient. The operation conditions used in these runs are presented in Table 6.

Table 7. Physical parameters used for simulating elution curves by pH and salt gradient

Parameter	Blue Sepharose	Protein A
Binding capacity (mg/mL)	5	50
Mean bead size (μm)	90	90
Macroporous diameter	300	300
Tortuosity	1.5	1.5
ϵ_b	0.3	0.3

broadening effect could be due to the possible glycosylation heterogeneity of the IgGs. This tail peak broadening is observed to a lesser extent for the IgG2b (Figure 5c). Estimated values for the parameters were used for simulating the elution curves of the three protein mixtures and mixtures of two proteins (Table 6, Figure 6). The model and the parameters estimated from single protein elution curves was able to predict the behaviour of almost all the protein mixture elution curves obtained with different pH gradient, flow rate and protein load. For all the mixtures the simulations followed quite closely the experimental results. In Figures 5 and 6, it can be seen that the model is able to predict very well the nonlinearity of the pH gradient that occurs experimentally. Table 7 shows the physical parameters used for simulating the elution curves for salt and pH gradients.

Conclusions

This paper has investigated the development of the necessary parameters to be used in a rationale to choose an optimal

separation sequence in order to include affinity chromatography. The mathematical modelling and simulation of such affinity systems has also been investigated. For the selection of operations two algorithms are used. In the first one the value of η , which corresponds to the efficiency (resolution) of the actual chromatography and, Σ , which determines the amount of a particular contaminant eliminated after each separation step, which determines the purity, have to be determined. It was found that the value of both these parameters is not generic for affinity separations but will depend on the type of affinity system used and will have to be determined on a case by case basis. η values of ca. 0.7 were found for Blue Sepharose and 0.9–1.0 for Protein A, which compare well with 1.0 for ion exchange and 0.86 for HIC determined previously. For Σ a value of 0.31 was obtained for Blue Sepharose and 0.22 for Protein A, which compare with 0.15 for ion exchange and 0.22 for HIC.

Mathematical modelling of both affinity systems using a rate model was carried out. With Blue Sepharose a salt gradient was used and with Protein A, a pH gradient. Parameters were determined with individual proteins and successful simulations of the protein mixtures were carried out. The largest deviation in the protein mixtures at different operating conditions was 8% for BSA and less for the IgGs. The 'tailing' effect observed on the right hand side of most peaks could be caused by the possible heterogeneity of the proteins due to glycosylation.

Acknowledgements

The authors acknowledge the Millenium Scientific Initiative for financial support (ICM-P05-001-F).

REFERENCES

- Asenjo, JA. 1990. Selection of operations in separation processes. In *Separation Processes in Biotechnology*, Asenjo JA (ed.) Marcel Dekker: New York; 3–16.
- Asenjo, JA Andrews, BA. 2004. Is there a rational method to purify proteins?: from expert systems to proteomics. *J. Mol. Recognit.* **17**: 236–247.
- Carroll, DL. 2009. D. L. Carroll's FORTRAN Genetic Algorithm Driver, <http://cuaerospace.com/carroll/ga.html> accessed in March 2009.
- Gu, T. 1995. *Mathematical Modeling and Scale-Up of Liquid Chromatography*. Berlin: Springer.
- Lazo, C. 1999. *Simulation of Liquid Chromatography and Simulated Moving Bed (SMB) Systems*. Suidienarbeit Technische Universitat: Hamburg-Harburg.
- Leser, EW. 1996. *Prot_Ex: an expert system for selecting the sequence of processes for the downstream purification of proteins*. Ph.D. Thesis, University of Reading.
- Leser, EW, Asenjo, JA. 1992. The rational design of purification processes for recombinant proteins. *J. Chromatogr.* **584**: 35–42.
- Li, W., Zhang, S., Sun, Y. 2004. Modeling of the linear-gradient dye-ligand affinity chromatography with a binary adsorption isotherm. *Biochem. Eng. J.* **22**: 63–70.
- Lienqueo, ME, Leser, EW, Asenjo JA. 1996. An expert system for the selection and synthesis of multistep protein separation processes. *Comput. Chem. Eng.* **20**: S189–S194.
- Orellana CA., Shene C., Asenjo JA. 2009. Mathematical modeling of elution curves for a protein mixture in ion exchange chromatography applied to high protein concentration. *Biotechnol. Bioeng.* **104**: 572–581.
- Shene C, Lucero A, Andrews BA, Asenjo, JA. 2006. Mathematical modeling of elution curves for a protein mixture in ion exchange chromatography and for the optimal selection of operational conditions. *Biotechnol. Bioeng.* **95**: 704–713.